Published in final edited form as:
J Proteome Res. 2010 October 1; 9(10): 5413–5421. doi:10.1021/pr100653r.

Mass Spectrometric Identification of Key Proteolytic Cleavage Sites in Statherin Affecting Mineral Homeostasis and Bacterial Binding Domains

Eva J. Helmerhorst, **Georges Traboulsi**, **Erdjan Salih**, and **Frank G. Oppenheim***
Department of Periodontology and Oral Biology, Henry M. Goldman School of Dental Medicine, 700 Albany Street, Boston, MA 02118

Abstract

Human salivary statherin inhibits both primary and secondary calcium phosphate precipitation and, upon binding to hydroxyapatite, associates with a variety of oral bacteria. These functions, crucial in the maintenance of tooth enamel integrity, are located in defined regions within the statherin molecule. Proteases associated with saliva, however, cleave statherin effectively, and it is of importance to determine how statherin functional domains are affected by these events. Statherin was isolated from human parotid secretion by zinc precipitation and purified by reversed-phase high performance liquid chromatography (RP-HPLC). To characterize the proteolytic process provoked by oral proteases, statherin was incubated with whole saliva and fragmentation was monitored by RP-HPLC. The early formed peptides were structurally characterized by reversed phase liquid chromatography electrospray-ionization tandem mass spectrometry. Statherin was degraded 3.6x faster in whole saliva than in whole saliva supernatant. The main and primary cleavage sites were located in the N-terminal half of statherin, specifically after Arg^{9}, Arg^{10}, and Arg^{13}; after Phe^{14} and Tyr^{18}; and after Gly^{12}, Gly^{15}, Gly^{17} and Gly^{19} while the C-terminal half of statherin remained intact. Whole saliva protease activities separated the charged N-terminus from the hydrophobic C-terminus, negatively impacting on full length statherin functions comprising enamel lubrication and inhibition of primary calcium phosphate precipitation. Cryptic epitopes for bacterial binding residing in the C-terminal domain were likewise affected. The full characterization of the statherin peptides generated facilitates the elucidation of their novel functional roles in the oral and gastro-intestinal environment.

Keywords

Oral; Enzymatic; Statherin; Fragmentation; Saliva

INTRODUCTION

Statherin is a human salivary protein produced by the parotid and submandibular glands. Originally discovered as a tyrosine-rich protein showing an unusually high affinity for hydroxyapatite 1 , statherin was one of the first salivary proteins to be isolated to purity and sequenced 2 . Statherin has an M_r of 5380 Da, consists of 43 amino acid residues and, besides tyrosine, is rich in proline and glutamic acid. In the C-terminal two thirds of the protein these amino acids occur in multiple repetitions of di- and tetrapeptide sequences, i.e. 4 × Gln-Pro, 3 × Tyr-Gln and 2 × Pro-Tyr-Gln-Pro. The N-terminal third of the molecule

*Address correspondence to: Frank G. Oppenheim, D.M.D., Ph.D., Dept. Periodontology and Oral Biology, Henry M. Goldman School of Dental Medicine, 700 Albany Street CABR W201, Boston, MA 02118, Phone: 617-638-4756, Fax: 617-638-4924, fropp@bu.edu.

contains more negatively than positively charged residues, rendering the protein acidic in nature with an IEP of 4.2 2 . Five consecutive acidic residues, one aspartic acid, two phosphoserines and two glutamic acid residues occupy positions 1 to 5 at the N-terminus.

As for many salivary proteins, statherin appears in several isoforms. Three variants have been identified in submandibular/sublingual secretions 3 . Variant SV2 represents an alternative splicing variant, lacking residues 6–15 encoded by exon 4. Variants SV1 and SV3 are post-translational cleavage products of statherin and SV2, respectively and both lack the C-terminal Phe residue. More recently, a novel statherin variant was discovered in whole saliva arising through intra-molecular cyclization after secretion by oral epithelial transglutaminase 2, linking Glu^{37} to Lys^{6} 4 . Average statherin concentrations in oral fluids have been determined by immuno-quantitation and were 4.3 μg/ml in whole saliva and 95.9, and 73.6 μg/ml in glandular parotid and submandibular/sublingual secretions, respectively 5 . The concentration differences between whole saliva and glandular secretions are significant and point to substantial post-secretory proteolytic processing of statherin, further increasing its structural diversity.

Polarity within the statherin structure with respect to charged and hydrophobic domains endows this protein with unique functional characteristics (summarized in Fig. 1). Due to its amphipathic nature, full length statherin exhibits the properties of a boundary lubricant, reducing frictional forces during mastication 6 . The hydroxyapatite binding properties of statherin are associated with the N-terminus as well its capacity to inhibit secondary (seeded) calcium phosphate precipitation 7 . Full length statherin furthermore inhibits spontaneous calcium phosphate precipitation, a property crucial for maintaining saliva supersaturated with respect to calcium and phosphate salts. When adsorbing to the tooth surface, the C-terminal domain undergoes transition from random coil to alpha-helical conformations 8, 9 , unmasking oral bacterial binding epitopes that were not accessible in the protein in solution 10–13 . Recently, statherin has been demonstrated to inhibit the conversion of *C. albicans* blastoconidia into the more virulent hyphal growth form 14 . Overall, statherin is important for oral health by protecting tooth enamel through lubrication and maintaining mineral homeostasis, and, in the adsorbed state, by contributing to the early phases of microbial colonization.

Because of the unique distribution of charged and hydrophobic residues and doubly phosphorylated N-terminus, chemical synthesis of statherin by solid phase techniques is challenging, although successful synthesis of full length statherin by F-moc chemistry has been reported 15. Recombinant expression of non-phosphorylated statherin in bacterial expression systems is feasible, but to obtain native statherin, phosphorylation of the N-terminal vicinal serine residues requires *in vitro* incubation with the appropriate Golgi casein kinase 16 . In the present study we report an optimized preparative isolation method to obtain statherin in pure form from human parotid secretion. The isolated material was used to study statherin fragmentation in whole saliva, a biological process frequently overlooked with regard to protein functionality in the oral cavity. The fragmentation cascade was biochemically characterized by RP-HPLC and LC-ESI-MS/MS. Cleavage in the identified regions may reveal a new vista on *in vivo* proteolysis of statherin and functional implications relevant to oral and gastro-intestinal health.

Methods

Saliva collection

Informed consent was obtained from all saliva donors prior to sample collection according to approved protocols of the Institutional Review Board at Boston University Medical Center. All enrolled subjects presented with good oral health without overt signs of gingival

inflammation or other oral conditions. Human parotid secretion (HPS) was collected from four healthy volunteers with the aid of a Curby cup positioned over the orifice of the Stensen's duct. HPS flow was stimulated with sour lemon candies (Jolly Rancher, Hershey's, PA) and the secretion was collected in graduated tubes placed on ice. Stimulated whole saliva (WS) was also collected on ice, from the same four subjects. A 5 ml aliquot was obtained between 10.00 and 11.00 AM at least 1 hour after the last meal. WS flow was stimulated by mastication on 4 square inches of Parafilm (American National Can™, Chicago, IL). After collection equal volumes of WS samples were pooled. To obtain WS supernatant (WSS), WS was cleared from particulate matter such as bacteria and host-derived cells by centrifugation at 14,000 × *g* for 20 min at 4° C. In some experiments, WSS was diluted ten fold in saliva ion buffer containing containing 50 mM KCl, 1.5 mM potassium phosphate, 1 mM $CaCl_2$, and 0.1 mM $MgCl_2$, pH 7.0 17.

Statherin isolation by zinc precipitation

Statherin was purified from freshly collected HPS by using the zinc precipitation method previously described 18 with several modifications. $ZnCl_2$ was added to 80 ml of HPS to a final concentration of 687.5 mM. The pH of the solution was adjusted to 9.0 with 2M NaOH, and the solution was incubated on ice for one hour. The precipitate formed was collected by centrifugation at 16,000 × g for 20 min at 4°C. Typically, sediments from 80 ml HPS starting material were dissolved in a total volume of 4 ml of 2% TFA. Minor undissolved particles were removed by centrifugation, dissolved in 0.2 ml of DMSO and analyzed separately.

Bis-Tris SDS PAGE

Pre-cast 12% Bis-Tris gels (Novex, InVitrogen, Carlsbad, CA) were used for SDS polyacrylamide gel electrophoresis (PAGE). Samples to be analyzed were boiled for 5 minutes in sample buffer containing 60 mM Tris-HCl, pH 6.8, 2.5% (w/v) glycerol, 2% (w/v) SDS, 0.1 M DTT and 0.1% (w/v) bromophenol blue. Electrophoresis was carried out in running buffer containing 25 mM Tris, 0.2 M glycine and 0.1% (w:v) SDS, pH 8.3 at a constant voltage of 120 V. The gels were stained with 0.1% (w/v) Coomassie Brilliant Blue R-250 in 40% (v/v) methanol and 10% (v/v) acetic acid for 16 hours followed by destaining in the same solution without dye.

Cationic PAGE

Proteins were dissolved in sample buffer containing 0.04% methyl green (Thermo Fisher, Waltham, MA) in 40% sucrose (Sigma, St. Louis, MO). Cationic proteins were separated by 15% cationic PAGE as previously described 19, 20 using the Bio-Rad mini-gel system and spacers of 1.5 mm thickness. Gel polymerization was accelerated by exposing the gels to a light source (60 Watts). Electrophoresis was carried out at a constant voltage of 120 V after which the gels were stained and destained as described above.

Anionic PAGE

Dried samples were resuspended in sample buffer containing 6% (v/v) HCl, 60 mM Tris, HCl, 1% (v/v) Temed, 20% sucrose, and 0.0008% (w/v) bromophenol blue. Electrophoresis was carried out as previously described 21, 22 using the Bio-Rad mini-gel system and spacers of 1.5 mm thickness. The separating gel contained 7.5% (w/v) acrylamide. After electrophoresis at 120 V, the proteins were stained with 0.5% (w/v) amido black 10B in 7% (v/v) glacial acetic acid, followed by destaining in 7% (v/v) glacial acetic acid.

Semi-preparative RP-HPLC for statherin isolation

The zinc precipitated proteins dissolved in 2% TFA were filtered through a 0.2 μm HT Tuffryn membrane filter (Pall Co., An Arbor, MI). The sample was subjected to RP-HPLC on a preparative C-18 column (TSK-GEL 5μm, ODT-120T, 7.8mm × 300mm, TOSOHaas, Montgomeryville, PA) connected to a HPLC apparatus (Model 715, Gilson, Middleton, WI). Proteins/peptides in the sample were eluted at a flow rate of 1.5 ml/min using a linear gradient generated from mixing buffer A containing 0.1% trifluoroacitic acid (TFA) and buffer B containing 80% acetonitrile and 0.1% TFA. The linear gradient used reached 55% buffer B after 74 minutes. Absorbance was monitored both at 219 nm and 230 nm. Proteins were collected using the peak collection mode with a peak width and peak sensitivity settings of 0.5 and 2.5, respectively (Unipoint 3.3 software, Gilson). Fractions were first flash evaporated under nitrogen (Glas-Col, Terre Haute, IN), redissolved in 0.5 ml of 50 mM ammonium bicarbonate buffer (pH 8.0) and lyophilized (FreezeMobile 25L, Virtis, SP Scientific, Gardiner, NY). Typically, 2 mg of statherin could be isolated from 80 ml HPS. The concentration of statherin in solution was determined spectrophotometrically at 215 nm using an extinction coefficient (ε) of $20.mg^{-1}.ml^{-1}$. Purity of the preparation was further verified by RP-HPLC with a very shallow gradient. The gradient consisted of the following segments: 0–10 minutes: 0–35% buffer B; 10–40 minutes: 35–46% buffer B; and 40–45 minutes: 46–100% buffer B. The identity of statherin in the collected peak was verified by ESI-MS in the static mode (see below).

Proteolysis of purified statherin in WS and WSS

For assessing statherin susceptibility to oral fluid proteases, statherin (400 μg/ml) was added to WS, WSS and to 1:10 diluted WSS. The incubation times selected for these experiments were: 0, 10, 30, 60 and 90 minutes for incubations in WS; 0, 1, 3, 5 and 7 hours for incubations in WSS and 0, 4, 8 and 24 h for incubations in 1:10 diluted WSS. All incubations were carried out at 37°C and 100 μl aliquots were removed at the indicated time points. The aliquots were boiled for 10 minutes, mixed with 900 μl buffer A and analyzed by analytical RP-HPLC.

Analytical RP-HPLC for monitoring statherin degradation

For analytical RP-HPLC samples were loaded onto a C-18 column of 4.6mm × 250mm. Proteins/peptides were eluted applying the same gradient from 0 to 55% buffer B over a 74 min time interval. In samples of statherin incubated in WS or WSS, the amount of residual intact statherin was quantitated by integration from the peak area relative to intact statherin. In samples of statherin incubated in 1:10 WSS peaks containing proteolytic products of statherin were collected, dried and characterized by LC-ESI-MS/MS.

Liquid chromatography electrospray ionization tandem mass spectrometry (LC-ESI-MS/MS

The purity of the statherin sample was analyzed by ESI-MS in the static mode using an LTQ-linear ion trap mass spectrometer (Thermo Electron, San Jose, CA). Fractions were dissolved in 20 μl of 50% acetonitrile and 0.1% formic acid. Samples were applied to a PicoTip emitter (New Objective, Woburn, MA) with a tip of 4 μm in diameter followed by ESI-MS using an electrospray voltage of 2.3 kV. Obtained spectra were deconvoluted using ProMass for XCalibur software (Thermo Finnigan). To structurally characterize statherin degradation fragments, lyophilized RP-HPLC fractions were dissolved in 20 μl of 2.5% acetonitrile and 0.1% formic acid and analyzed by LC-ESI-MS/MS. The raw MS data were searched using Bioworks software (version 3.3.1) against a database containing the 43 residue statherin (Swissprot accession number P02808) and the 33 residue statherin variant SV2. The selected filter criteria were 1) “no enzyme”; 2) DeltaCN ≥ 0.1; 3) peptide probability ≤ 0.05, XCorr score value ≥ 2.2 and 3.5 for $z = 2$ and 3, respectively. Among the

total number of peptides sequenced in a particular fraction, the most frequently observed fragment was considered the main constituent. In most fractions one peptide was clearly predominant representing more than 90% of all peptides sequenced.

RESULTS

PAGE analysis of HPS and zinc precipitates

In order to maximize the precipitation of statherin from human parotid secretion, the molarity of added zinc chloride was increased to 687.5 μM. Dissolution of the precipitate was accomplished in 2% TFA in 1/20th of the original volume of HPS. Most of the zinc precipitated proteins dissolved well in 2% TFA. Some undissolved material was removed by centrifugation, and this minor fraction was dissolved in DMSO. The compositions of HPS, HPS supernatant, the zinc precipitate dissolved in 2% TFA and the second precipitate dissolved in DMSO were subjected to various PAGE systems including Bis-Tris PAGE, cationic PAGE and a nionic PAGE (Fig. 2). These three electrophoretic systems separate proteins based on size, size and positive charges and size and negative charges, respectively. Amounts applied from each of the fractions originated from the same volume of HPS. Bis-Tris PAGE analysis showed that zinc chloride effectively precipitated the small molecular weight protein fraction from HPS (Fig. 2A; lane 3). This lane also contained a minor component with a molecular weight of approximately 37 kD which may represent proline-rich glycoprotein 23 . The molecular weight of the TFA-insoluble protein in lane 4 was about 55 kD in size, possibly representing a non-glycosylated isoform of amylase 24 . Cationic PAGE was performed to visualize histatins20, 25 . Results indicated the presence of histatins 1, 3, and 5 in the zinc precipitate and their complete disappearance from the supernatant, (Fig. 2B; lanes 2 and 3). Neutral and negatively charged proteins in the zinc precipitate were observed by anionic PAGE by which the major salivary proline-rich protein isoforms can be separated 21, 26, 27 . In HPS and HPS supernatant, two double bands were noted (indicated with arrows) representing proline-rich proteins (PRPs); PRP1, PIF-s and PRP2 in the upper double band and PRP3, PIF-f and PRP4 in the lower double bands (Fig. 2C) 27 . The PRPs appeared to remain in the supernatant and not to precipitate with zinc chloride. Anionic PAGE of the TFA-dissolved pellet showed histatin 1 (white arrow) which, due to its neutral pH, can be visualized in the anionic PAGE system 28 . Lane 3 also displays statherin (dotted arrow) and some minor other bands indicating the necessity for further RP-HPLC purification of the zinc precipitate.

RP-HPLC and ESI-MS analysis of zinc precipitates and statherin

The zinc-precipitated proteins dissolved in 2% TFA were subjected to reverse phase high performance liquid chromatography (RP-HPLC). Chromatograms of samples from three individual subjects display almost identical component compositions (Fig. 3). The four major peaks contained histatin 5, histatin 3, histatin 1 and statherin 18 . Levels of histatins and statherin differed between subjects and these individual differences were confirmed by repeat collections from the same donors (data not shown). The data also showed that the statherin levels were consistently somewhat below that of the three histatins. The major statherin peak was collected and subjected to shallow gradient RP-HPLC, confirming the purity of the preparation (Fig. 4). The statherin preparations before and after shallow gradient RP-HPLC were also compared by anionic PAGE (Fig. 3C, lanes 5 and 6) indicating they were electrophoretically identical. ESI-MS analysis of the statherin peak revealed a pattern characteristic of the pure statherin protein carrying 5+, 4+ and 3+ charges (Fig. 5A). No additional peaks of unknown m/z values were observed. The deconvoluted average nominal mass was 5380.4 Da, closely matching the theoretical mass of 5299.8 Da of full length phosphorylated statherin. The data indicate that a single RP-HPLC separation step of the zinc precipitated HPS proteins was sufficient to obtain statherin in pure form.

Statherin proteolysis in WS and WSS

There is ample evidence that certain salivary proteins are susceptible to degradation by whole saliva proteases (reviewed in 29). While proteolytic rates differ between subjects, a remarkable consistency in protease specificities has been reported, justifying the use of pooled human whole saliva in degradation experiments 30, 31 . To obtain average rates, statherin was added to pooled WS or WSS and incubated for various time intervals (0–90 min in WS and 0–7 hr in WSS). The time points selected were chosen to capture the complete proteolysis of statherin in WS and in WSS, respectively. A relatively high concentration of statherin was added. This facilitated the detection of statherin protein by RP-HPLC above WS/WSS protein background levels, which typically exhibited minimal absorbance in the statherin peak region. In addition, at this added concentration of statherin it can be assumed that oral proteases operate at maximum velocity (V_{max}) making it feasible to compare between WS and WSS rates. As a control, statherin was added to WS and WSS which had been boiled to abolish protease activities. Statherin degradation in WS and WSS was monitored by RP-HPLC (Fig. 6A and 6D, respectively) and quantitated from the statherin peak area in the chromatogram (Fig. 6B and 6E, respectively). Half the added amount of statherin disappeared in WS after 26 minutes and in WSS after 1.5 h, indicating that proteolytic rates in WS were 3.6 fold higher than in WSS. In boiled WS and WSS statherin remained intact (Fig. 6C and 6F, respectively).

Characterization of primary proteolytic cleavage sites

Further degradation experiments were carried out with 1:10 diluted WSS to further reduce the absorbance by endogenous statherin peptides to undetectable levels. Statherin was added and sample aliquots were removed and analyzed after 0h, 4h, 8h and 24h of incubation (Fig. 7A). As proteolysis progressed, the intact statherin peak (P6) gradually decreased concomitant with the appearance of statherin fragments (peaks P1 to P5). The elution diagram from 0–50 min and beyond 74 min gave no evidence for additional peptides (not shown). LC-ESI-MS/MS analysis of P1–P5 indicated that without exception all cleavages of statherin had occurred in the N-terminal half of the protein (Fig. 7B). In this domain, all peptide bonds C-terminal to glycine residues (Gly^{12}, Gly^{15}, Gly^{17} and Gly^{19}) and arginines (Arg^{9}, Arg^{10}, and Arg^{13}) were hydrolyzed. In addition, cleavages were noted after Phe^{14} and Tyr^{18}, but not after Phe^{7} and any of the other tyrosine residues. The most abundant peptides were those resulting from cleavage after Arg^{9}, Arg^{10}, Arg^{13} and Phe^{14} . Noticeably, no cleavage after Lys^{6} had occurred, pointing to preferential cleavage of Arg but not Lys residues. The hydrophobic C-terminus of statherin appeared to survive, at least in the initial phases, proteolysis by oral fluid associated enzymes.

DISCUSSION

Statherin was successfully isolated from HPS by zinc precipitation and RP-HPLC. ESI-MS of the main statherin peak in the chromatogram showed no evidence for any of the three statherin variants, SV1, SV2 or SV3, indicating that the approach is suitable to obtain statherin without the closely resembling isoforms at a preparative level. The three isoforms of statherin were originally discovered and isolated from submandibular/sublingual secretion3. Two of these variants, SV1 and SV2, have recently been found in parotid salivary secretion as well31 . In the original study, the variants were separated from statherin by RP-HPLC at a gradient increase of 0.8% B/min. This is comparable to the gradient applied in our studies (0.7% B/min) and a similar resolution can be expected. We observed small peaks in the chromatogram of the zinc precipitate eluting prior to the main statherin peak in the RP-HPLC chromatograms (Fig. 3), possibly representing statherin variants. The aim of this study however was to obtain pure full length statherin, which was achieved with the optimized methodology described.

Evidence for the fragmentation of statherin in whole saliva has been presented in prior peptidome studies 17, 31–33 . What has not been accomplished before is to unravel and define the early time sequence of statherin fragmentation and evaluate the primary cleavage sites targeted by oral proteases. We found in human pooled diluted WSS that the N-terminal half of the molecule is attacked first. All peptide bonds C-terminal to glycines were hydrolyzed pointing to distinct enzymatic specificities. Prominent cleavages were furthermore observed after Arg^{9}, Arg^{10}, Arg^{13}, and Phe^{14} . Interestingly, while cleavage was observed after Phe^{14}, the other Phe residue in the N-terminal domain, Phe^{7}, was not targeted. Likewise, Tyr^{18} was cleaved but not Tyr^{16} suggesting specificity for cleavage of certain hydrophobic residues in a defined context. Tyrosine residues in the hydrophobic part of the molecule, Tyr^{21}, Tyr^{30}, Tyr^{34}, Tyr^{38} and Tyr^{41} were all untouched, further emphasizing that cleavage after Tyr^{16} was specific. It is of interest to note that statherin variants SV2 and SV3, lacking the segment spanning residues 6–15 containing Arg^{9}, Arg^{10} , Arg^{13}, Phe^{14}, Gly^{12} and Gly^{15} (Fig. 1) has substantially fewer candidate cleavage sites than intact statherin. Consequently, SV2 can be expected to be less susceptible than statherin to proteolysis in the oral cavity. Overall, the C-terminus of native statherin was resistant to proteolysis in the time span examined. Smaller statherin fragments, however, resulting from cleavages in this domain have been detected, in WS as well as in the acquired enamel pellicle 34,35 , indicating additional cleavages may occur at later stages in the *in vivo* statherin fragmentation process.

Enzymes responsible for the proteolytic degradation of statherin in whole saliva fluid have yet to be identified. To gain insight into the molecular weight of the statherin-degrading enzymes, we have attempted a zymography approach in which statherin was incorporated into the acrylamide gel system as the enzymatic substrate. In our previous studies this technique was succesfully applied to investigate the proteases cleaving histatins, another group of small molecular weight salivary proteins 36 . In the histatin zymogram gels we could determine that the major proteolytic enzymes cleaving histatins were 50–75kD in size. Some of the active proteases were identified by in gel trypsinization and LC-ESI-MS/MS as lactotransferrin, kallikrein-1, and human airway trypsin-like protease. Unfortunately, the zymography approach with statherin was unsuccessful, perhaps because of significant differences in primary structure and isoelectric points between histatins and statherin and resultant differences in their immobilization in the gel during the polymerization/ electrophoresis process. As for histatins, we demonstrated for statherin that most of the involved proteolytic enzymes are cell associated, based on the fact that the enzymatic activity was almost four fold higher in WS than in WSS. The identification of bacterial enzymes in the cell pellet remains a challenge due to the current limitations in the number of established bacterial genomes and the low levels at which bacterial enzymes are present in saliva.

From a biological perspective, statherin exhibits a number of functions that are highly important to the maintenance of oral health. As summarized in Fig. 1, these functions are in some cases assigned to selective domains within the statherin structure, whereas for other functions, intact statherin is required. Proteolysis may abolish statherin's capacity to inhibit primary calcium phosphate precipitation and lubrication, properties associated with the full length molecule. It also could interfere with statherin ability to bind *C. albicans* and to inhibit yeast to hyphae conversion which are associated with full length statherin and residues 6–43, respectively 14 . On the other hand, based on our data it can be anticipated that inhibition of secondary calcium phosphate precipitation, a function previously localized in residues 1–6, would be unaffected. Another important function residing in the N-terminus of statherin is adherence to the tooth surface and participation in the formation of the acquired enamel pellicle1, 37 . Previous isothermal titration microcalorimetry and adsorption isotherm measurements have distinguished two phases in the adsorption process

of statherin to hydroxyapatite 8 . The initial low coverage binding step involves A-type sites on the crystal lattice and is exothermic in nature. Subsequent binding provokes higher coverage, occurs at B-type sites and appears to be thermodynamically neutral. Solid NMR analysis has shown that once statherin binds to a mineral surface, a conformational change is induced in the C-terminus, adopting an alpha-helical conformation 9 . These conformational changes are thought to expose hidden epitopes. Such epitopes were originally referred to as “cryptitopes” and first described in salivary proline-rich proteins38 . Revelation of epitopes in statherin upon adsorption to the tooth surface facilitates binding of certain oral bacteria such as *A. viscosus* and *P. gingivalis* 10, 12 . Proteolytic cleavage of statherin at the N-terminus implies that the hydroxyapatite binding regions become separated from the C-terminal region. Consequently, adsorption-induced conformational changes in the C-terminal domain are not anymore likely to occur when the N-terminus is cleaved off. Hence, statherin fragmentation in the oral cavity could prevent bacterial binding to cryptic epitopes in the C-terminal domain.

Recently it has been shown that adsorption to hydroxyapatite reduces the sensitivity of histatin 1 to oral fluid proteases 39 . Histatin 1 and statherin share many physical characteristics; both are about 5 kD in size, are phosphorylated and exhibit affinity for hydroxyapatite. In analogy to the observations made with histatin 1, it can be speculated that statherin adsorption to hydroxyapatite may reduce proteolytic susceptibility. The here identified primary fragmentation sites in statherin are located in a region immediately adjacent to the N-terminal hydroxyapatite binding domain. Upon binding of statherin to the enamel surface, the protease susceptible domain spanning residues Lys^{6}-Gly^{19} could become less accessible to proteolytic enzymes, for instance as a result of steric hindrance or conformational changes induced in the adsorbed statherin molecule. This is relevant since statherin binds with high affinity to hydroxyapatite 40 , and the rate of adsorption likely outcompetes the rate of statherin proteolysis in whole saliva.

In conclusion, fragmentation of statherin by oral enzymes is clearly generating multiple fragments for which functional roles have not yet been established. Of particular interest is the survival of the C-terminal statherin domain, which may underscore the essentiality of this part of the molecule for biological functions. Given the structural characterization of the preponderant statherin peptides, novel functions are now amenable to characterization.

Supplementary Material

Refer to Web version on PubMed Central for supplementary material.

Acknowledgments

The authors thank Dr. Xiuli Sun and Nerline Grand-Pierre for technical assistance. The studies were supported by the National Institutes of Health/National Institute of Dental and Craniofacial Research grants DE18132 (EJH), AI087803 (EJH), DE18448 (ES), DE05672 (FGO) and DE07652 (FGO).

Abbreviations used

HPS	human parotid secretion
TFA	trifluoroacetic acid
DTT	dithiothreitol
LC-ESI-MS/MS	liquid chromatography electro spray ionization tandem mass spectrometry

RP-HPLC	reversed phase high performance liquid chromatography
WS	whole saliva
WSS	whole saliva supernatant

REFERENCES

1. Hay DI. The isolation from human parotid saliva of a tyrosine-rich acidic peptide which exhibits high affinity for hydroxyapatite surfaces. Arch Oral Biol. 1973; 18(12):1531–1541. [PubMed: 4522816]
2. Schlesinger DH, Hay DI. Complete covalent structure of statherin, a tyrosine-rich acidic peptide which inhibits calcium phosphate precipitation from human parotid saliva. J Biol Chem. 1977; 252(5):1689–1695. [PubMed: 838735]
3. Jensen JL, Lamkin MS, Troxler RF, Oppenheim FG. Multiple forms of statherin in human salivary secretions. Arch Oral Biol. 1991; 36(7):529–534. [PubMed: 1663737]
4. Cabras T, Inzitari R, Fanali C, Scarano E, Patamia M, Sanna MT, Pisano E, Giardina B, Castagnola M, Messana I. HPLC-MS characterization of cyclo-statherin Q-37, a specific cyclization product of human salivary statherin generated by transglutaminase 2. J Sep Sci. 2006; 29(17):2600–2608. [PubMed: 17313100]
5. Li J, Helmerhorst EJ, Yao Y, Nunn ME, Troxler RF, Oppenheim FG. Statherin is an in vivo pellicle constituent: identification and immuno-quantification. Arch Oral Biol. 2004; 49(5):379–385. [PubMed: 15041485]
6. Douglas WH, Reeh ES, Ramasubbu N, Raj PA, Bhandary KK, Levine MJ. Statherin: a major boundary lubricant of human saliva. Biochem Biophys Res Commun. 1991; 180(1):91–97. [PubMed: 1718282]
7. Hay DI, Moreno EC, Schlesinger DH. Phosphoprotein-inhibitors of calcium phosphate precipitation from salivary secretions. Inorg Perspec Biol Med. 1979; 2:271–285.
8. Goobes G, Goobes R, Shaw WJ, Gibson JM, Long JR, Raghunathan V, Schueler-Furman O, Popham JM, Baker D, Campbell CT, Stayton PS, Drobny GP. The structure, dynamics, and energetics of protein adsorption-lessons learned from adsorption of statherin to hydroxyapatite. Magn Reson Chem. 2008; 45(S1):S32–S47. [PubMed: 18172904]
9. Goobes G, Goobes R, Schueler-Furman O, Baker D, Stayton PS, Drobny GP. Folding of the C-terminal bacterial binding domain in statherin upon adsorption onto hydroxyapatite crystals. Proc Natl Acad Sci U S A. 2006; 103(44):16083–16088. [PubMed: 17060618]
10. Amano A, Shizukuishi S, Horie H, Kimura S, Morisaki I, Hamada S. Binding of Porphyromonas gingivalis fimbriae to proline-rich glycoproteins in parotid saliva via a domain shared by major salivary components. Infect Immun. 1998; 66(5):2072–2077. [PubMed: 9573091]
11. Li T, Johansson I, Hay DI, Stromberg N. Strains of Actinomyces naeslundii and Actinomyces viscosus exhibit structurally variant fimbrial subunit proteins and bind to different peptide motifs in salivary proteins. Infect Immun. 1999; 67(5):2053–2059. [PubMed: 10225854]
12. Niemi LD, Johansson I. Salivary statherin peptide-binding epitopes of commensal and potentially infectious Actinomyces spp. delineated by a hybrid peptide construct. Infect Immun. 2004; 72(2): 782–787. [PubMed: 14742521]
13. Sekine S, Kataoka K, Tanaka M, Nagata H, Kawakami T, Akaji K, Aimoto S, Shizukuishi S. Active domains of salivary statherin on apatitic surfaces for binding to Fusobacterium nucleatum cells. Microbiology. 2004; 150(Pt 7):2373–2379. [PubMed: 15256578]
14. Leito JT, Ligtenberg AJ, Nazmi K, Veerman EC. Identification of salivary components that induce transition of hyphae to yeast in Candida albicans. FEMS Yeast Res. 2009; 9(7):1102–1110. [PubMed: 19799638]
15. Gururaja TL, Levine MJ. Solid-phase synthesis and characterization of human salivary statherin: a tyrosine-rich phosphoprotein inhibitor of calcium phosphate precipitation. Pept Res. 1996; 9(6): 283–289. [PubMed: 9048421]

16. Manconi B, Cabras T, Vitali A, Fanali C, Fiorita A, Inzitari R, Castagnola M, Messana I, Sanna MT. Expression, purification, phosphorylation and characterization of recombinant human statherin. Protein Expr Purif. 2010; 69(2):219–225. [PubMed: 19651217]

17. Helmerhorst EJ, Sun X, Salih E, Oppenheim FG. Identification of Lys-Pro-Gln as a novel cleavage site specificity of saliva-associated proteases. J Biol Chem. 2008; 283(29):19957–19966. [PubMed: 18463091]

18. Flora B, Gusman H, Helmerhorst EJ, Troxler RF, Oppenheim FG. A new method for the isolation of histatins 1, 3, and 5 from parotid secretion using zinc precipitation. Protein Expr Purif. 2001; 23(1):198–206. [PubMed: 11570863]

19. Baum BJ, Bird JL, Longton RW. Histidine-rich-polypeptides in Macaque parotid saliva are not nuclear histones. Arch Oral Biol. 1977; 22(7):455–456. [PubMed: 413534]

20. Campese M, Sun X, Bosch JA, Oppenheim FG, Helmerhorst EJ. Concentration and fate of histatins and acidic proline-rich proteins in the oral environment. Arch Oral Biol. 2009; 54(4): 345–353. [PubMed: 19159863]

21. Davis BJ. Disc Electrophoresis. Ii. Method And Application To Human Serum Proteins. Ann N Y Acad Sci. 1964; 121:404–427. [PubMed: 14240539]

22. Oppenheim FG, Offner GD, Troxler RF. Phosphoproteins in the parotid saliva from the subhuman primate Macaca fascicularis. Isolation and characterization of a proline-rich phosphoglycoprotein and the complete covalent structure of a proline-rich phosphopeptide. J Biol Chem. 1982; 257(16): 9271–9282. [PubMed: 7107568]

23. Reddy MS, Levine MJ, Tabak LA. Structure of the carbohydrate chains of the proline-rich glycoprotein from human parotid saliva. Biochem Biophys Res Commun. 1982; 104(3):882–888. [PubMed: 7073733]

24. Scannapieco FA, Torres G, Levine MJ. Salivary alpha-amylase: role in dental plaque and caries formation. Crit Rev Oral Biol Med. 1993; 4(3–4):301–307. [PubMed: 8373987]

25. Baum BJ, Bird JL, Longton RW. Polyacrylamide gel electrophoresis of human salivary histidine-rich-polypeptides. J Dent Res. 1977; 56(9):1115–1118. [PubMed: 270513]

26. Ornstein L. Disc Electrophoresis. I. Background And Theory. Ann N Y Acad Sci. 1964; 121:321–349. [PubMed: 14240533]

27. Hay DI, Ahern JM, Schluckebier SK, Schlesinger DH. Human salivary acidic proline-rich protein polymorphisms and biosynthesis studied by high-performance liquid chromatography. J Dent Res. 1994; 73(11):1717–1726. [PubMed: 7983258]

28. Oppenheim FG, Yang YC, Diamond RD, Hyslop D, Offner GD, Troxler RF. The primary structure and functional characterization of the neutral histidine-rich polypeptide from human parotid secretion. J Biol Chem. 1986; 261(3):1177–1182. [PubMed: 3944083]

29. Helmerhorst EJ, Oppenheim FG. Saliva: a dynamic proteome. J Dent Res. 2007; 86(8):680–693. [PubMed: 17652194]

30. Helmerhorst EJ, Alagl AS, Siqueira WL, Oppenheim FG. Oral fluid proteolytic effects on histatin 5 structure and function. Arch Oral Biol. 2006; 51(12):1061–1070. [PubMed: 16901460]

31. Messana I, Cabras T, Pisano E, Sanna MT, Olianas A, Manconi B, Pellegrini M, Paludetti G, Scarano E, Fiorita A, Agostino S, Contucci AM, Calo L, Picciotti PM, Manni A, Bennick A, Vitali A, Fanali C, Inzitari R, Castagnola M. Trafficking and postsecretory events responsible for the formation of secreted human salivary peptides: a proteomics approach. Mol Cell Proteomics. 2008; 7(5):911–926. [PubMed: 18187409]

32. Vitorino R, Barros A, Caseiro A, Domingues P, Duarte P, Amado F. Towards defining the whole salivary peptidome. Prot Clin Appl. 2009; 3:528–540.

33. Huq NL, Cross KJ, Ung M, Myroforidis H, Veith PD, Chen D, Stanton D, He H, Ward BR, Reynolds EC. A review of the salivary proteome and peptidome and saliva-derived peptide therapeutics. Prot Clin Appl. 2007; 13:547–564.

34. Siqueira WL, Zhang W, Helmerhorst EJ, Gygi SP, Oppenheim FG. Identification of protein components in in vivo human acquired enamel pellicle using LC-ESI-MS/MS. J Proteome Res. 2007; 6(6):2152–2160. [PubMed: 17447804]

35. Vitorino R, Calheiros-Lobo MJ, Duarte JA, Domingues PM, Amado FM. Peptide profile of human acquired enamel pellicle using MALDI tandem MS. J Sep Sci. 2008; 31(3):523–537. [PubMed: 18266264]

36. Sun X, Salih E, Oppenheim FG, Helmerhorst EJ. Activity-based mass spectrometric characterization of proteases and inhibitors in human saliva. Proteomics Clin Appl. 2009; 3(7): 810–820. [PubMed: 20011683]

37. Raj PA, Johnsson M, Levine MJ, Nancollas GH. Salivary statherin. Dependence on sequence, charge, hydrogen bonding potency, and helical conformation for adsorption to hydroxyapatite and inhibition of mineralization. J Biol Chem. 1992; 267(9):5968–5976. [PubMed: 1313424]

38. Gibbons RJ, Hay DI, Schlesinger DH. Delineation of a segment of adsorbed salivary acidic proline-rich proteins which promotes adhesion of Streptococcus gordonii to apatitic surfaces. Infect Immun. 1991; 59(9):2948–2954. [PubMed: 1879920]

39. McDonald E, Goldberg HA, Tabbara N, Mendes FM, Siqueira WL. Histatin 1 resists proteolytic environment when adsorbed to hydroxyapatite. J Dent Res. 2010 in press.

40. Moreno EC, Kresak M, Hay DI. Adsorption of molecules of biological interest onto hydroxyapatite. Calcif Tissue Int. 1984; 36(1):48–59. [PubMed: 6423236]

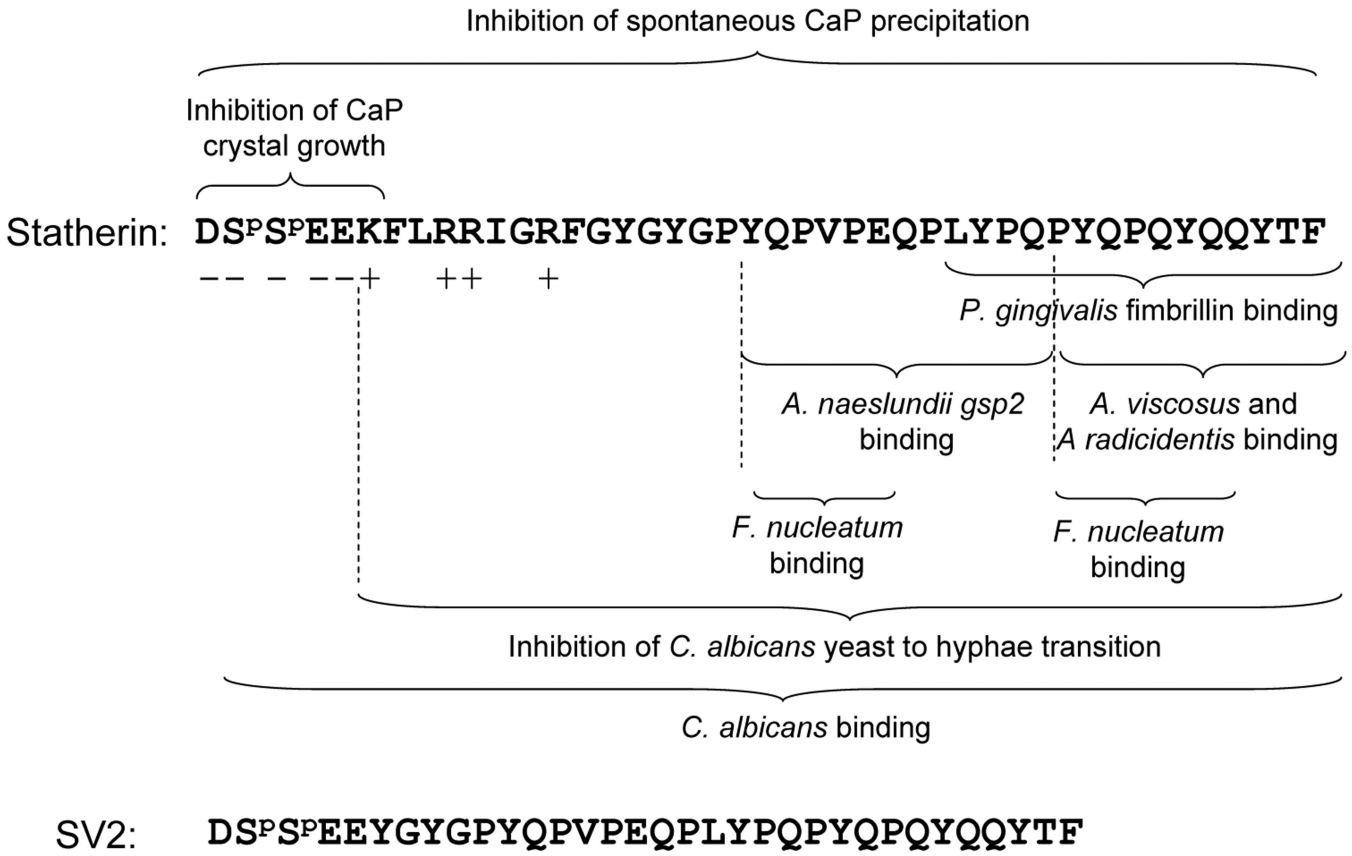

Fig. 1.
Structural and functional characteristics of statherin.

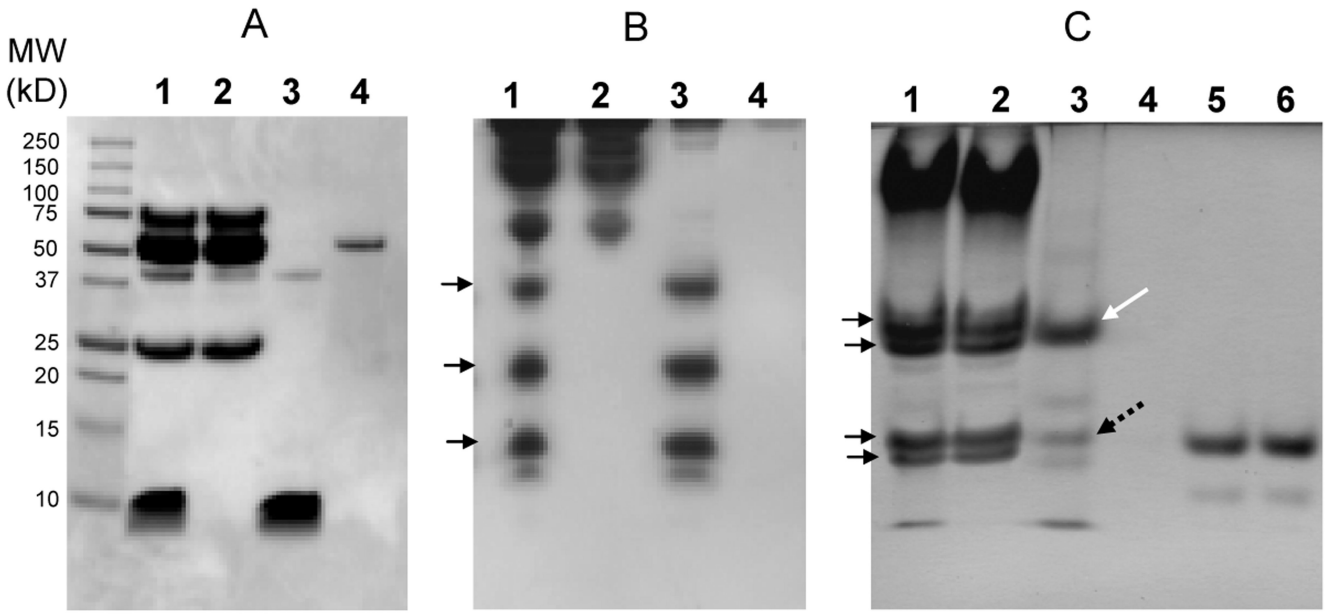

Fig. 2.

PAGE analysis of human parotid secretion (HPS) and zinc-precipitated proteins. A, SDS PAGE; B, cationic PAGE; C, anionic PAGE. Gel A far left lane: molecular weight (MW) standard (Bio-Rad). All gels: lane 1, HPS (100 μl); lane 2: HPS supernatant after zinc-precipitation (100 ul); lane 3: zinc-precipitated proteins from 100 μl HPS, soluble in 2% TFA; lane 4: TFA-insoluble zinc precipitated proteins from 100 μl HPS dissolved in DMSO. Arrows in gel B point from top to bottom to the positions of histatins 1, 3, and 5, respectively. Arrows in gel C point to the acidic proline-rich proteins (see text for details). Gel C lane 5: statherin purified by RP-HPLC (20 μg); lane 6: statherin after further purification by isocratic RP-HPLC (20 μg).

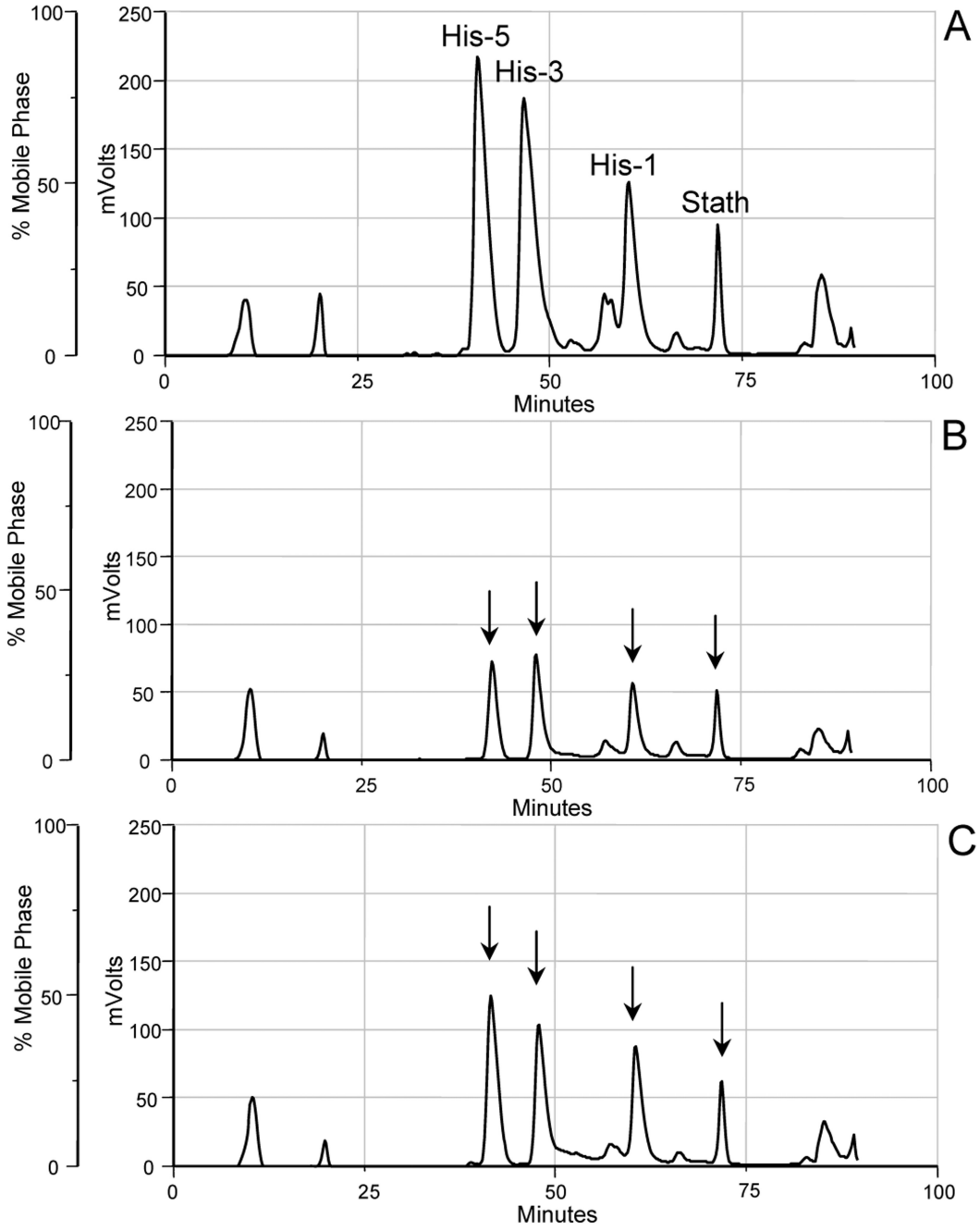

Fig. 3.

RP-HPLC analysis of proteins from HPS precipitated with zinc chloride. A, B, and C: results obtained for three individual HPS donors. The zinc-chloride precipitated material in all three subjects contained primarily histatins 5, 3, 1 and statherin.

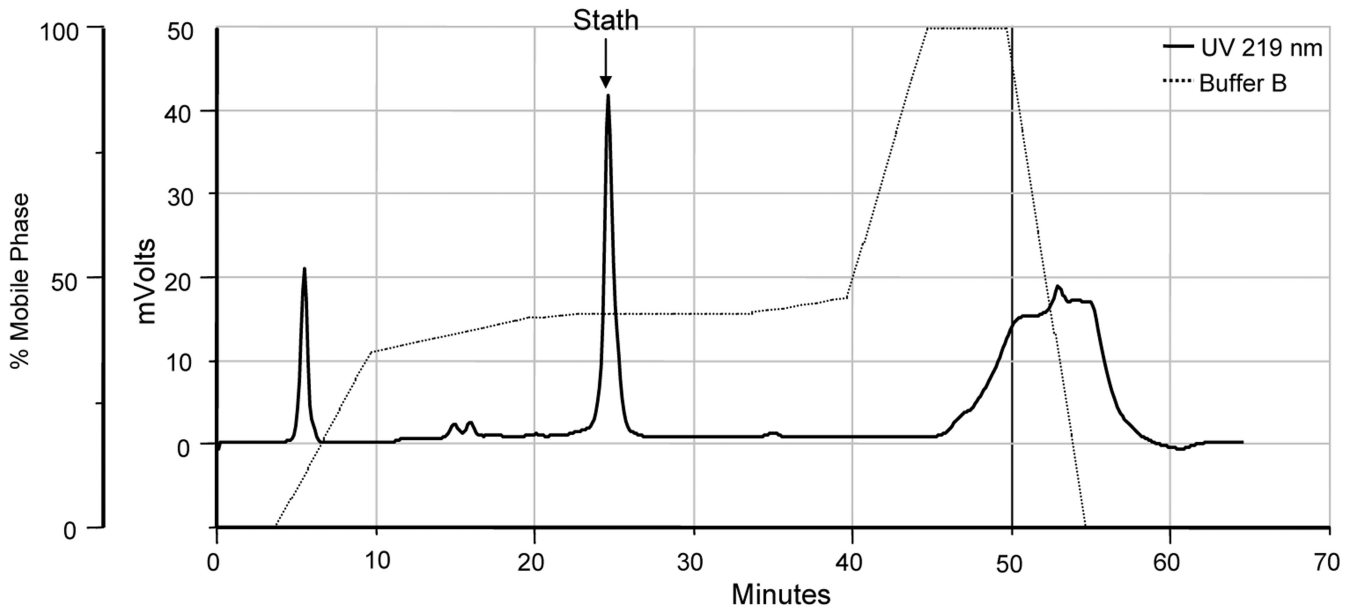

Fig. 4.
Isocratic RP-HPLC analysis of the pooled statherin peak.

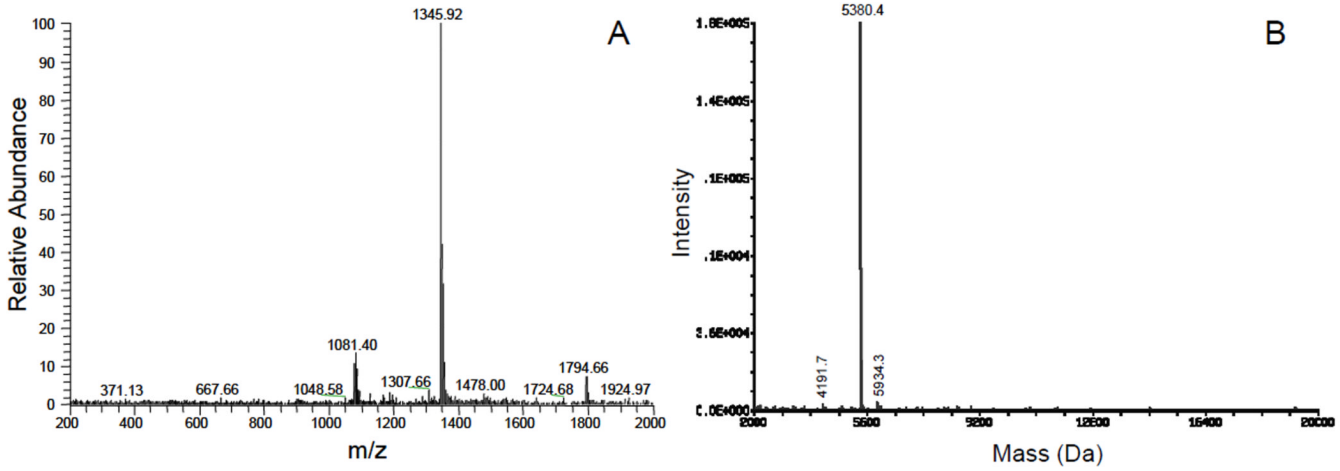

Fig. 5.

ESI-MS analysis of the pooled statherin peak. A, MS spectrum showing multiple charged species of statherin; B. Deconvoluted mass of statherin (5380.4 Da).

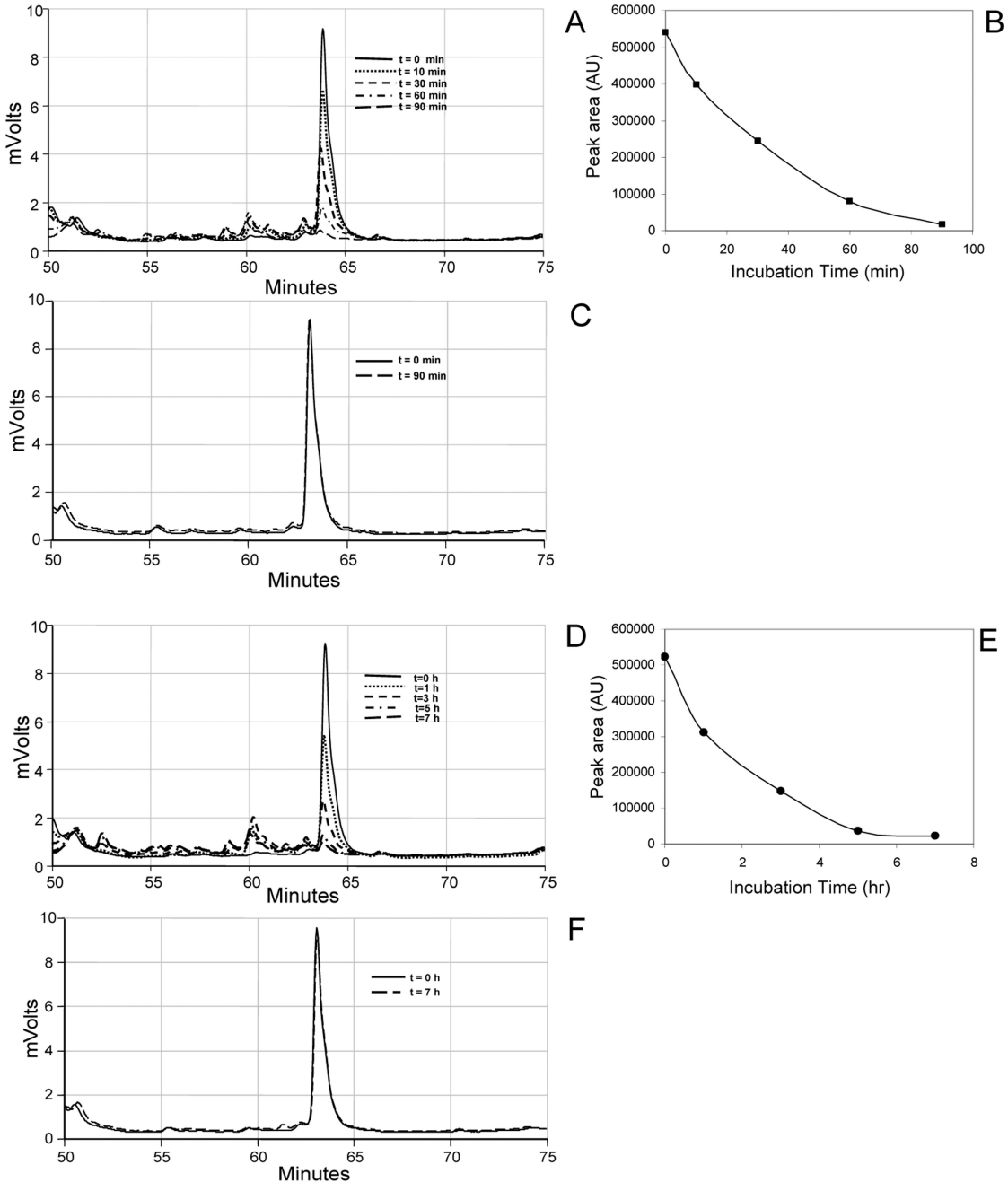

Fig. 6.

Degradation of statherin in WS and WSS. Statherin was added to a final concentration of 400 μg/ml to pooled human WS or WSS. After various time intervals, 100 μl aliquots were removed, boiled and analyzed by RP-HPLC. A and D, statherin incubated with WS and WSS, respectively; B and D, plots of statherin peak areas in WS and WSS, respectively; C and F, statherin incubated with boiled WS and WSS, respectively (control).

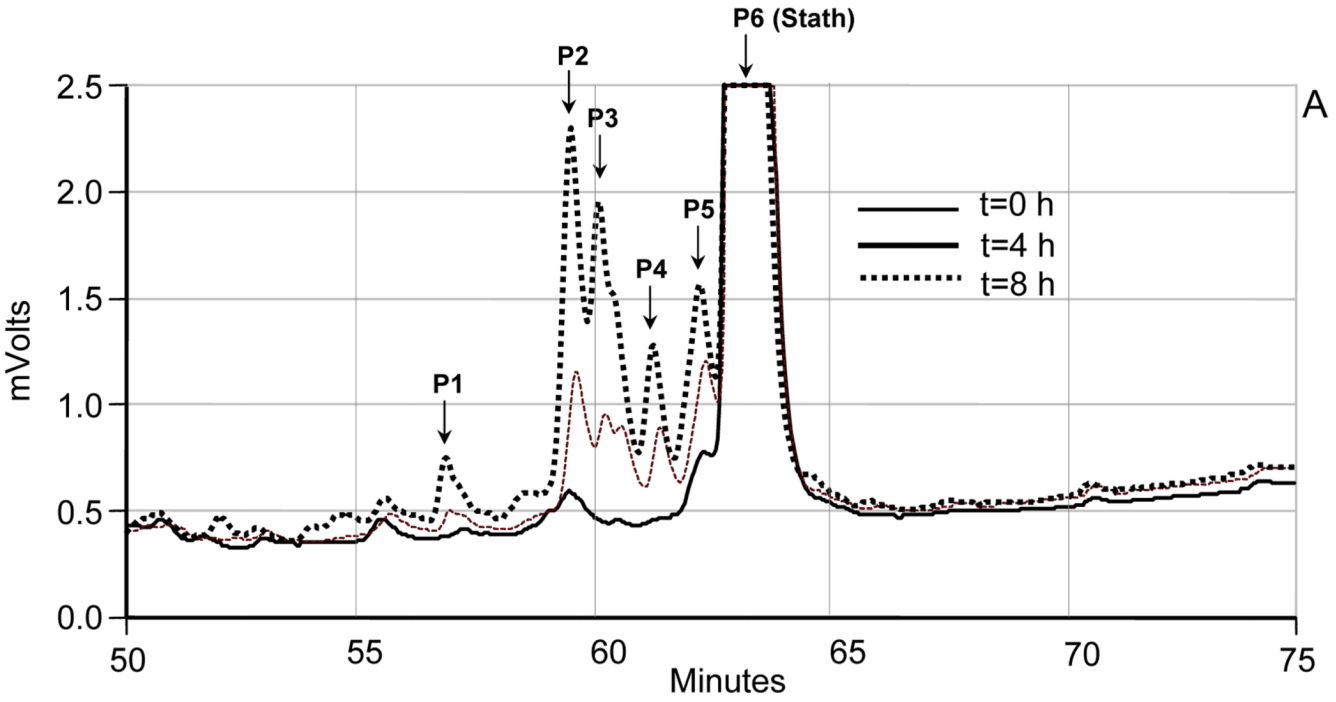

B

Present in Peak	Peptides identified	Cleaved after
P1	GPYQPVPEQPLYPQPYQPQYQQYTF	Tyr^{18}
P2	YGPYQPVPEQPLYPQPYQPQYQQYTF	Gly^{17}
P2,P3	GYGYGPYQPVPEQPLYPQPYQPQYQQYTF	Phe^{14}
P3	YGYGPYQPVPEQPLYPQPYQPQYQQYTF	Gly^{15}
P4,P5	RFGYGYGPYQPVPEQPLYPQPYQPQYQQYTF	Gly^{12}
P4,P5	RIGRFGYGYGPYQPVPEQPLYPQPYQPQYQQYTF	Arg^{9}
P5	IGRFGYGYGPYQPVPEQPLYPQPYQPQYQQYTF	Arg^{10}
P5	FGYGYGPYQPVPEQPLYPQPYQPQYQQYTF	Arg^{13}
P5	PYQPVPEQPLYPQPYQPQYQQYTF	Gly^{19}
Stath	DSSEEKFLRRIGRFGYGYGPYQPVPEQPLYPQPYQPQYQQYTF	

Fig. 7.

Degradation of statherin in 1:10 diluted WSS and characterization of the major degradation fragments. Statherin was added to a final concentration of 400 μg/ml to 1:10 diluted pooled human WSS. After various time intervals, 100 μl aliquots were removed, boiled and subjected to RP-HPLC. A, zoom of the RP-HPLC chromatogram magnifying the elution time frame of the statherin degradation fragments; B, amino acid sequences of the degradation fragments determined by LC-ESI-MS/MS.